A Robust Multi-market Bidding Strategy for BESS

Sunho Jang, Siddharth Bhela, and Nan Xue

***Abstract*— Distributed Battery Energy Storage Systems (BESS) have the potential to offer significant grid services and generate revenue for their owners. In this paper, we propose a novel robust BESS planning algorithm designed to maximize revenues by bidding in multiple ancillary service markets under uncertainties. The proposed algorithm enables BESS to provide frequency regulation and synchronized reserve markets while concurrently fulfilling commitments to a long-term capacity market without violating any operational constraints. In addition, the proposed algorithm is robust to uncertainties within the system, particularly in frequency regulation signal and synchronized reserve events. To makes the solvable optimization problem, we provide a Mixed-Integer Linear Programming (MILP) reformulation of the original problem by leveraging Lagrange dual functions. Experiment results demonstrate that the proposed algorithm is robust to the given uncertainties and outperforms two selected benchmarks.**

I. Introduction

As the penetration of intermittent renewable energy generation continues to surge, the role of Battery Energy Storage Systems (BESS) has become important for ensuring grid resiliency. With their rapid ramping capabilities, ESSs can deal with the fluctuations in renewable energy generation by offering various services to the grid. Many independent system operators, such as PJM, incentivize the owners of the BESS to provide ancillary services by the revenues from the ancillary service markets, and hence reduce the electricity cost. There has been a body of work on optimal operations of BESS to maximize the profits by energy arbitrage [1]–[3], peak-shaving [4], frequency regulation [5], [6], and joint optimization of multiple ancillary services [7]–[9].

However, scheduling those bids to the ancillary service markets is challenging since we cannot precisely predict in advance how much BESS's capacity will be available for those ancillary services. This is mainly due to the uncertainty within the net power consumption of a BESS, when it is providing an ancillary service, is governed by some unpredictable signals or events (e.g., frequency regulation signal, synchronized reserve events). This necessitates an algorithm that bids an appropriate amount of BESS's capacity to each ancillary service market that can be provided as planned for any possible uncertainties.

In this paper, we propose a robust look-ahead BESS scheduling algorithm that bids the BESS to multiple ancillary services markets under various uncertainties. We consider a scenario where the BESS has already been committed to a long-term capacity market, and the owner of BESS makes bids to the frequency regulation and synchronized reserve market whenever the BESS is not expected to be called for its commitment to the long-term capacity market.

This work was supported by ....

Several previous studies have focused on BESS energy arbitrage algorithms that are robust against the given uncertainties [10], [11] or satisfy chance constraints on BESS operation [12]. Ref. [13] presents a robust strategy that jointly optimizes both energy arbitrage and reactive power service. Nevertheless, these works do not provide a robust solution for providing multiple ancillary services.

Some works such as [7], [14] have proposed a framework for robust co-optimization of energy arbitrage and multiple ancillary services including frequency regulation. Ref. [8] has proposed a joint optimization framework for BESS planning that deals with the uncertainties in frequency regulation signals using a scenario-based approach. Ref. [15] proposes a data-driven distributionally robust chance-constrained BESS bidding strategy to deal with the uncertainties within frequency regulation signals. However, the approaches from these works do not guarantee robustness against the uncertainties within frequency regulation signals and do not consider long-term capacity market.

In comparison to existing literatures, the contributions of our work are:

1) We introduce a novel look-ahead BESS planning algorithm to the ancillary service markets when BESS has been committed to a long-term capacity market. The provided algorithm is robust against uncertainties not only from variable load profiles and solar PV generation, but also from the frequency regulation signal and synchronized reserve events.
2) We utilize uncertainty budgets to describe the uncertainty within the ancillary service signals, which curtails excessive conservatism in the robust algorithm.

This paper is organized as follows. Section II introduces the setting, including the constraints and the cost function, for the look-ahead ancillary service scheduling optimization. Section III proposes reformulation of the robust optimization problem into a solvable form. Section IV demonstrates the result experiments where we compare the proposed algorithm with two benchmarks. Section V provides the conclusion of the paper.

Notation: For sets A and B, $A \times B$ is the cartesian product of them. The notation $(x)^+$ refers to $\max\{x, 0\}$. We write $\boldsymbol{x} \succeq c$ if every element of vector $\boldsymbol{x}$ is larger than or equal to c.

II. Problem Formulation

In this section, we introduce the look-ahead robust BESS scheduling that bids a Battery Energy Storage System

(BESS) to the frequency regulation market and synchronized reserve market. We demonstrate the models for the BESS and the ancillary service markets, which form the constraints and objective of robust scheduling optimization. We assume that the look-ahead scheduling is conducted for a finite prediction horizon composed of T discrete intervals with length Δt, indexed by $t \in \mathcal{T} := \{1, \ldots, T\}$. The period of look-ahead scheduling optimization is generic and depends on the problem in interest. Our problem of interest specifically considers a day-ahead hourly scheduling, i.e., Δt is equal to 1 hour and T is equal to 24.

A. BESS Model

We consider a large-scale BESS and denote the State of Charge (SoC) at time step t by E_t^{B}. The SoC evolves as follows

$$E_{t+1}^{\mathrm{B}} = E_t^{\mathrm{B}} + \eta_c P_t^{\mathrm{C}} - \frac{1}{\eta_d} P_t^{\mathrm{D}} \qquad \forall t \in \mathcal{T}, \tag{1}$$

where P_t^{C} and P_t^{D} are average charging and discharging power at the time step t, η_c and η_d are charging and discharging efficiencies, respectively. The BESS is not allowed to simultaneously charge and discharge:

$$0 \le P_t^{\mathrm{C}} \le \mu_t \overline{P}^{\mathrm{C}} \qquad \forall t \in \mathcal{T} \tag{2}$$

$$0 \le P_t^{\mathrm{D}} \le (1 - \mu_t) \overline{P}^{\mathrm{D}} \qquad \forall t \in \mathcal{T}, \tag{3}$$

where $\overline{P}^{\mathrm{C}}$ is the maximum charging power, $\overline{P}^{\mathrm{D}}$ is the maximum discharging power, and μ_t is 1 if the BESS is charging, and 0 otherwise. Hence, the BESS's net power consumption P_t^{N} has the following relationship with P_t^{C} and P_t^{D} :

$$P_t^{\mathrm{N}} = P_t^{\mathrm{C}} - P_t^{\mathrm{D}} \qquad \forall t \in \mathcal{T} \tag{4}$$

$$P_t^{\mathrm{C}} = \max\left\{P_t^{\mathrm{N}}, 0\right\} \qquad \forall t \in \mathcal{T} \tag{5}$$

$$P_t^{\mathrm{D}} = -\max\left\{-P_t^{\mathrm{N}}, 0\right\} \qquad \forall t \in \mathcal{T}. \tag{6}$$

Due to the different coefficients for P_t^{C} and P_t^{D} in (1), the SoC E_t^{B} is a non-convex and nonlinear function of $P_1^{\mathrm{N}}, \ldots, P_{t-1}^{\mathrm{N}}$.

It is shown that BESS degradation of BESS is significantly accelerated if it is overly charged or discharged [16], [17]. To prevent quick BESS degradation, we keep the SoC inside the range $[\underline{E}^{\mathrm{B}}, \overline{E}^{\mathrm{B}}]$:

$$\underline{E}^{\mathrm{B}} \le E_t^{\mathrm{B}} \le \overline{E}^{\mathrm{B}} \qquad \forall t \in \mathcal{T} \tag{7}$$

B. Building/Microgrid

The BESS is installed in a building or a microgrid with a solar PV system. The imported power from the grid to the building P_t^{G} is given as

$$P_t^{\mathrm{G}} = P_t^{\mathrm{N}} + P_t^{\mathrm{PV}} - P_t^{\mathrm{UC}} \qquad \forall t \in \mathcal{T}, \tag{8}$$

where P_t^{PV} is the PV generation power, and P_t^{UC} is the load from the building. The PV generation P_t^{PV} and the load P_t^{UC} cannot be exactly known in advance and considered as uncertainties in the phase.

C. Ancillary Service Markets

We consider a scenario that the BESS is committed to a long-term capacity market, which requires it tSo be fully chargedS when it is called by the Independent System Operator (ISO). To prevent the BESS from being on standby all the time, the building owner uses a service from a third-party company that provides predictions on ISO's call times which are assumed to be accurate in this work. While the BESS cannot provide any ancillary services when it is called by the ISO, it can make revenues by engaging in other ancillary services on periods during when the ISO's call is not anticipated. In this work, we make an offer to two ancillary service markets for that duration: frequency regulation market, synchronized reserve market.

Suppose that the BESS is expected to be called by the ISO during the set of time steps $\mathcal{T}_{\mathrm{F}} \subseteq \mathcal{T}$ and the first time step is t_{F}. The BESS must be fully charged to its maximum SoC $\overline{E}^{\mathrm{B}}$ at t_{F} and maximize its discharging power during the time steps in $\mathcal{T}_{\mathrm{F}}$:

$$E_{t_{\mathrm{F}}}^{\mathrm{B}} = \overline{E}^{\mathrm{B}} \tag{9}$$

$$P_t^{\mathrm{N}} = -\overline{P}^{\mathrm{D}} \qquad \forall t \in \mathcal{T}_{\mathrm{F}}. \tag{10}$$

Due to the constraint (9), the net power consumption at $t_{\mathrm{F}}-1$ is as follows

$$P_{t_{\mathrm{F}}-1}^{\mathrm{N}} = \frac{\overline{E}^{\mathrm{B}} - E_{t_{\mathrm{F}}-1}}{\eta_c}, \tag{11}$$

Since $P_{t_{\mathrm{F}}-1}^{\mathrm{N}}$ must be lower than $\overline{P}^{\mathrm{C}}$, the following must hold

$$E_{t_{\mathrm{F}}-1}^{\mathrm{B}} \ge \overline{E} - \eta_c \overline{P}^{\mathrm{C}}. \tag{12}$$

As described above, BESS's net power consumption must be manually controlled during the time steps in $\mathcal{T}_{\mathrm{F}}^{+} := \mathcal{T}_{\mathrm{F}} \cup \{t_{\mathrm{F}} - 1\}$. Thus, it cannot provide any other ancillary services during $\mathcal{T}_{\mathrm{F}}^{+}$ and we must bids to the other ancillary markets only for the time steps in $\mathcal{T}_{\mathrm{S}} := \mathcal{T} \setminus \mathcal{T}_{\mathrm{F}}^{+}$.

The BESS submits an offer to the frequency regulation market that includes the baseline power P_t^{B} and the regulation capability P_t^{FR}. While the BESS is providing frequency regulation service, its net power consumption is adjusted by the frequency regulation signal from the ISO. To capture the feature of the regulation signal that is issued in a shorter period than the period Δt (e.g., 2 seconds in PJM), we define sub-intervals that breaks each time step t into D pieces with length $\Delta d := \Delta t / D$, indexed by d. We denote the frequency regulation signal at each sub-interval by $s_{t,d} \in [-1, 1]$; also, the average regulation signal $s_{t,d}$ during the time step t is denoted by s_t with only one subscript. Then, the BESS's net power is as follows

$$P_{t,d}^{\mathrm{N}} = P_t^{\mathrm{B}} - s_{t,d} P_t^{\mathrm{FR}}.$$

The net power $P_{t,d}^{\mathrm{N}}$ must be in the range $[-\overline{P}^{\mathrm{D}}, \overline{P}^{\mathrm{C}}]$ for any $s_{t,d} \in [-1, 1]$, which leads to the following inequality

$$0 \le P_t^{\mathrm{FR}} \le \alpha_t \frac{\overline{P}^{\mathrm{C}} + \overline{P}^{\mathrm{D}}}{2} \qquad \forall t \in \mathcal{T}_{\mathrm{S}}, \tag{13}$$

where α_t is 1 when the BESS schedules to bid to the frequency regulation market, and 0 otherwise.

For the synchronized reserve market, we schedule a day-ahead offer that includes the baseline power P_t^{B} and the amount of synchronized reserve P_t^{SR}. While the BESS is providing the synchronized reserve service, the BESS's net power is adjusted as follows

$$P_{t,d}^{\mathrm{N}} = P_t^{\mathrm{B}} - r_{t,d} P_t^{\mathrm{SR}},$$

where $r_{t,d} \in [0,1]$ is the fraction of synchronized reserve called by the ISO; r_t denotes the average of $r_{t,d}$ for all $d \in \{1,\ldots,D\}$. Similar to (13), we get the following inequality

$$0 \le P_t^{\mathrm{SR}} \le \beta_t \left(\overline{P}^{\mathrm{C}} + \overline{P}^{\mathrm{D}} \right) \qquad \forall t \in \mathcal{T}_{\mathrm{S}}. \tag{14}$$

The BESS cannot simultaneously provide both the frequency regulation and synchronized reserve service at each time step, which corresponds to the following:

$$\alpha_t + \beta_t \le 1 \qquad \forall t \in \mathcal{T}_{\mathrm{S}}. \tag{15}$$

Since either P_t^{FR} or P_t^{SR} must be zero, the net power of the BESS can be written as follows

$$P_t^{\mathrm{N}} = P_t^{\mathrm{B}} - s_t P_t^{\mathrm{FR}} - r_t P_t^{\mathrm{SR}} \qquad \forall t \in \mathcal{T}_{\mathrm{S}} \tag{16}$$

In addition, the maximum charging and discharging power (i.e., when $s_{t,d} = 1$ or -1, $r_{t,d} = 1$ in (16)) during the ancillary services must not exceed $\overline{P}^{\mathrm{C}}$ and $\overline{P}^{\mathrm{D}}$:

$$P_t^{\mathrm{B}} + P_t^{\mathrm{FR}} \le \overline{P}^{\mathrm{C}} \qquad \forall t \in \mathcal{T}_{\mathrm{S}} \tag{17}$$

$$-P_t^{\mathrm{B}} + P_t^{\mathrm{FR}} + P_t^{\mathrm{SR}} \le \overline{P}^{\mathrm{D}} \qquad \forall t \in \mathcal{T}_{\mathrm{S}}. \tag{18}$$

Note that, the regulation signal s_t and the utilized synchronized reserve r_t cannot be precisely known in advance, and thus considered as uncertainties in the look-ahead .

D. Uncertainty Description

There are four uncertainties during the scheduling: frequency regulation signal $\boldsymbol{s} := (s_1,\ldots,s_T)$, reserve fraction $\boldsymbol{r} := (r_1,\ldots,r_T)$, PV generation $\boldsymbol{P}^{\mathrm{PV}} := (P_1^{\mathrm{PV}},\ldots,P_T^{\mathrm{PV}})$, and building's load $\boldsymbol{P}^{\mathrm{UC}} := (P_1^{\mathrm{UC}},\ldots,P_T^{\mathrm{UC}})$. We define the uncertainty sets for each of these by leveraging the robust parameters called uncertainty budgets as follows

$$\mathcal{S} = \left\{ \boldsymbol{s} \;\middle|\; s_t \in [\underline{s}, \overline{s}],\ \underline{\Gamma}_t^{\mathrm{s}} \le \sum_{k=1}^{t} s_k \le \overline{\Gamma}_t^{\mathrm{s}} \quad \forall t \in \mathcal{T} \right\} \tag{19}$$

$$\mathcal{R} = \left\{ \boldsymbol{r} \;\middle|\; r_t \in [\underline{r}, \overline{r}],\ \underline{\Gamma}_t^{\mathrm{r}} \le \sum_{k=1}^{t} r_k \le \overline{\Gamma}_t^{\mathrm{r}} \quad \forall t \in \mathcal{T} \right\} \tag{20}$$

$$\mathcal{P}^{\mathrm{PV}} = \left\{ \boldsymbol{P}^{\mathrm{PV}} \;\middle|\; P_t^{\mathrm{PV}} \in \left[\underline{P}_t^{\mathrm{PV}}, \overline{P}_t^{\mathrm{PV}}\right], \underline{\Gamma}_t^{\mathrm{PV}} \le \sum_{k=1}^{t} P_k^{\mathrm{PV}} \le \overline{\Gamma}_t^{\mathrm{PV}} \ \forall t \in \mathcal{T} \right\} \tag{21}$$

$$\mathcal{P}^{\mathrm{UC}} = \left\{ \boldsymbol{P}^{\mathrm{UC}} \;\middle|\; P_t^{\mathrm{UC}} \in \left[\underline{P}_t^{\mathrm{UC}}, \overline{P}_t^{\mathrm{UC}}\right], \underline{\Gamma}_t^{\mathrm{UC}} \le \sum_{k=1}^{t} P_k^{\mathrm{UC}} \le \overline{\Gamma}_t^{\mathrm{UC}} \ \forall t \in \mathcal{T} \right\}, \tag{22}$$

where the parameters $\underline{\bullet}$, $\overline{\bullet}$ are the bounds on each element of the uncertainties, and $\underline{\Gamma}_t^{\bullet}$, $\overline{\Gamma}_t^{\bullet}$ are the uncertainty budgets for each uncertainty. The bounds on s_t and r_t can be obtained from historical data, while the bounds on P_t^{PV} and P_t^{UC} are assumed to be predicted. Uncertainty budgets of those sets can be chosen by investigating the range of cumulative sums of the historical data. We gather all the uncertainties $\boldsymbol{w} := \{\boldsymbol{s}^\top, \boldsymbol{r}^\top, \boldsymbol{P}^{\mathrm{PV}\top}, \boldsymbol{P}^{\mathrm{UC}\top}\}^\top$ and define uncertainty set $\mathcal{W} := \mathcal{S} \times \mathcal{R} \times \mathcal{P}^{\mathrm{PV}} \times \mathcal{P}^{\mathrm{UC}}$.

E. Cost

The total cost includes four components: energy charge, peak demand charge, ancillary service revenues, and BESS degradation cost. The energy charge is paid to the utility given by

$$J^{\mathrm{E}} = \pi^{\mathrm{E}} \sum_{t=1}^{T} P_t^{\mathrm{G}} \cdot \Delta t, \tag{23}$$

where π^{E} is the fixed-rate cost for unit energy contracted with the utility and Δt is the length of a time step.

The building also pays the peak demand charge that is proportional to the maximum imported power P_t^{G} during a certain time period, practically a month. However, the prediction horizon for the look-ahead planning optimization is much shorter than a month and the precise cost cannot be precisely included in the cost function. Instead, we penalize the maximum power during the prediction horizon with a pre-defined weight π^{DC} as follows

$$J^{\mathrm{DC}} = \pi^{\mathrm{DC}} \max_{t \in \mathcal{T}} P_t^{\mathrm{G}}. \tag{24}$$

The revenue from ancillary services are proportional to the reserve provided to each market P_t^{FR} and P_t^{SR}. Hence, the revenue during the horizon is given by

$$J^{\mathrm{AC}} = \sum_{t=1}^{T} \pi_t^{\mathrm{FR}} P_t^{\mathrm{FR}} + \pi_t^{\mathrm{SR}} P_t^{\mathrm{SR}}, \tag{25}$$

where π_t^{FR} and π_t^{SR} are the predicted day-ahead unit power price at the frequency regulation and synchronized reserve markets, respectively. The prices π_t^{FR} and π_t^{SR} cannot be known in advance but we assume that we can precisely forecast them.

Lastly, we include the BESS degradation cost that is critical to the operation of a BESS. We use a cost model used in many previous works (e.g., [18] and [8]) where the cost is proportional to the absolute value of the net power P_t^{N} as follows

$$J^{\mathrm{BD}} = \pi^{\mathrm{BD}} \sum_{t=1}^{T} \left| P_t^{\mathrm{N}} \right|. \tag{26}$$

where π^{BD} is the cost per unit power computed as

$$\pi^{\mathrm{BD}} = \frac{\pi^{\mathrm{Cell}}}{2 N_{\mathrm{cyc}} \left(\overline{E}^{\mathrm{B}} - \underline{E}^{\mathrm{B}} \right)}, \tag{27}$$

where π^{Cell} is the price of the battery cell, N_{cyc} is the number of cycles the BESS can operate within the SoC range $[\underline{E}^{\text{B}}, \overline{E}^{\text{B}}]$. Then, the total cost J^{T} is computed as follows

$$J^{\text{T}} = J^{\text{E}} + J^{\text{DC}} - J^{\text{AC}} + J^{\text{BD}}. \tag{28}$$

F. Robust Look-ahead scheduling optimization

We formulate the robust look-ahead scheduling optimization that decides the look-ahead offers to the ancillary service markets P_t^{B}, P_t^{FR}, P_t^{SR}, α_t, β_t for all $t \in \mathcal{T}_{\text{S}}$:

$$\begin{aligned} &\min_{\boldsymbol{x}} \ \max_{\boldsymbol{w}\in\mathcal{W}} J^{\text{T}} \\ &\text{s.t. } (1)-(28) \qquad \forall \boldsymbol{w} \in \mathcal{W}, \end{aligned} \tag{29}$$

where $\boldsymbol{x} := (P_t^{\text{B}}, P_t^{\text{FR}}, P_t^{\text{SR}}, \alpha_t, \beta_t)_{t\in\mathcal{T}_{\text{S}}}$ is the vector of the decision variables. Note that the variables P_t^{N},P_t^{C},P_t^{D},P_t^{G}, E_t^{B} are dependent of $\boldsymbol{w}$, and hence are treated as uncertainties in the problem.

Due to the infinite number of uncertainties, the inequality constraints on the uncertainties must be reformulated into a set of a finite number of constraints for the optimization problem to be solvable. The constraints (2) and (3) trivially hold for all uncertainties if (4)-(6) and (16)-(18) is incorporated as constraints. However, (7) and (12) do not trivially hold for all possible uncertainties, and hence need a reformulation. In the next section, we derive a set of finite linear inequalities, which is a sufficient condition for (7) and (12), and use them in the reformulation of (29).

III. Reformulation of robust optimization

In this section, we propose a reformulation of (29) with a finite number of constraints. We first derive sufficient condition for (7), (12) using the bounds on E_t^{B}, which are demonstrated in Proposition 1 later. These sufficient conditions are tighten further as a set of finite linear inequalities by leveraging Lagrange dual functions. Finally, with an approximated and tractable cost function, we propose a MILP reformulation of the original problem (29).

A. Derivation of a Sufficient Condition

We start with writing the robust version of (7) and (12). The net power consumption of the BESS P_t^{N} depends on the regulation signal s_t and the reserve call r_t, and hence the SoC E_t^{B} depends on them as well. Thus, the robust version of (7) and (12) is written as follows

$$\min_{\boldsymbol{s}\in\mathcal{S},\boldsymbol{r}\in\mathcal{R}} E_t^{\text{B}} \geq \underline{E}^{\text{B}} \qquad \forall t \in \mathcal{T}\setminus\{t_{\text{F}}\} \tag{30}$$

$$\max_{\boldsymbol{s}\in\mathcal{S},\boldsymbol{r}\in\mathcal{R}} E_t^{\text{B}} \leq \overline{E}^{\text{B}} \qquad \forall t \in \mathcal{T}\setminus\{t_{\text{F}}\} \tag{31}$$

$$\min_{\boldsymbol{s}\in\mathcal{S},\boldsymbol{r}\in\mathcal{R}} E_{t_{\text{F}}-1}^{\text{B}} \geq \overline{E}^{\text{B}} - \eta_c \overline{P}^{\text{C}}. \tag{32}$$

Note that the time step t_{F} is not considered in (30) and (31) since $E_{t_{\text{F}}}$ is fixed as $\overline{E}^{\text{B}}$ by (9). To derive a sufficient condition of (30)-(32), we use the following proposition.

Proposition 1. *Suppose that P_t^{Du} is an auxiliary variable which satisfies*

$$P_t^{\text{Du}} \geq \left(-P_t^{\text{B}} + \overline{s}P_t^{\text{FR}} + \overline{r}P_t^{\text{SR}}\right)^+ \qquad \forall t \in \mathcal{T}, \tag{33}$$

and E_t^l and E_t^u are defined as

$$E_t^l = \begin{cases} E_1^B + \sum_{k=1}^{t-1} \eta_c P_k^N - \left(\frac{1}{\eta_d} - \eta_c\right) P_k^{Du} & \text{if } t < t_F \\ \overline{E}^B + \sum_{k=t_F}^{t-1} \eta_c P_k^N - \left(\frac{1}{\eta_d} - \eta_c\right) P_k^{Du} & \text{if } t \geq t_F \end{cases} \tag{34}$$

$$E_t^u = \begin{cases} E_1^B + \sum_{k=1}^{t-1} \eta P_k^N & \text{if } t < t_F \\ \overline{E}^B + \sum_{k=t_F}^{t-1} \eta P_k^N & \text{if } t \geq t_F, \end{cases} \tag{35}$$

where η is a constant in range $[\eta_c, 1/\eta_d]$. Then, the following inequality holds

$$E_t^{\text{l}} \leq E_t^{\text{B}} \leq E_t^{\text{u}} \qquad \forall t \in \mathcal{T}. \tag{36}$$

Proof. The inequality $E_t^{\text{B}} \leq E_t^{\text{u}}$ has already been proved in [19]. Hence, we show only the lower bound condition $E_t^{\text{l}} \leq E_t^{\text{B}}$.

First, P_t^{Du} is larger than P_t^{D} by the assumption (33) and (16). Now, we show $E_t^{\text{l}} \leq E_t^{\text{B}}$ by mathematical induction for any $t < t_{\text{F}}$. We first get $E_1^{\text{l}} \leq E_1^{\text{B}}$ from (34) so the statement holds for $t = 1$. Now suppose that $E_t^{\text{l}} \leq E_t^{\text{B}}$ holds. Then, we obtain the following for any $t < t_{\text{F}}$

$$\begin{aligned} E_{t+1}^{\text{B}} &= E_1^{\text{B}} + \sum_{k=1}^{t-1} \eta_c P_k^{\text{C}} - \frac{1}{\eta_d} P_k^{\text{D}} \\ &= E_1^{\text{B}} + \sum_{k=1}^{t-1} \eta_c \left(P_k^{\text{C}} - P_k^{\text{D}}\right) - \left(\frac{1}{\eta_d} - \eta_c\right) P_k^{\text{D}} \\ &\geq E_1^{\text{l}} + \sum_{k=1}^{t-1} \eta_c P_k^{\text{N}} - \left(\frac{1}{\eta_d} - \eta_c\right) P_k^{\text{Du}} = E_{t+1}^{\text{l}}. \end{aligned} \tag{37}$$

By the principle of mathematical induction, $E_t^{\text{l}} \leq E_t^{\text{B}}$ holds for $t < t_{\text{F}}$ and the inequality (36) holds. In a similar way, we can show $E_t^{\text{l}} \leq E_t^{\text{B}}$ for any $t \geq t_{\text{F}}$. Thus, the statement of the proposition holds. □

As a result of Proposition 1, the following conditions are sufficient conditions for (30), (31), and (32), respectively, under the assumption (33):

$$\min_{\boldsymbol{s}\in\mathcal{S},\boldsymbol{r}\in\mathcal{R}} E_t^{\text{l}} \geq \underline{E}^{\text{B}} \qquad \forall t \in \mathcal{T}\setminus\{t_{\text{F}}\} \tag{38}$$

$$\max_{\boldsymbol{s}\in\mathcal{S},\boldsymbol{r}\in\mathcal{R}} E_t^{\text{u}} \leq \overline{E}^{\text{B}} \qquad \forall t \in \mathcal{T}\setminus\{t_{\text{F}}\} \tag{39}$$

$$\min_{\boldsymbol{s}\in\mathcal{S},\boldsymbol{r}\in\mathcal{R}} E_{t_{\text{F}}-1}^{\text{l}} \geq \overline{E}^{\text{B}} - \eta_c \overline{P}^{\text{C}} \tag{40}$$

We again derive a sufficient condition of (38), (39) and (40) by leveraging the Lagrange dual functions $g_t^{\text{l}}(\boldsymbol{\lambda}_t^{\text{l}})$ and $g_t^{\text{u}}(\boldsymbol{\lambda}_t^{\text{u}})$ of $\min_{\boldsymbol{s}\in\mathcal{S},\boldsymbol{r}\in\mathcal{R}} E_t^{\text{l}}$ and $\max_{\boldsymbol{s}\in\mathcal{S},\boldsymbol{r}\in\mathcal{R}} E_t^{\text{u}}$, where $\boldsymbol{\lambda}_t^{\text{l}}$ and $\boldsymbol{\lambda}_t^{\text{u}}$ are the vectors composed of the Lagrange multipliers, respectively; these functions are derived in Appendix V-A.

Proposition 2. *Suppose that the following holds*

$$\boldsymbol{\lambda}_t^l \geq 0, \quad \boldsymbol{\lambda}_t^u \geq 0, \qquad \forall t \in \mathcal{T}\setminus\{t_F\} \tag{41}$$

$$g_t^l\left(\boldsymbol{\lambda}_t^l\right) \geq \underline{E}^B, \quad g_t^u\left(\boldsymbol{\lambda}_t^u\right) \leq \overline{E}^B \qquad \forall t \in \mathcal{T}\setminus\{t_F\} \tag{42}$$

$$g_{t_F-1}^l\left(\boldsymbol{\lambda}_{t_F-1}^l\right) \geq \overline{E}^B - \eta_c \overline{P}^C. \tag{43}$$

Then, the inequalities (38), (39), (40) hold.

Proof. By the property of Lagrange dual function [20], we have the following for any $\boldsymbol{\lambda}_t^{\mathrm{l}} \succeq 0$, $\boldsymbol{\lambda}_t^{\mathrm{u}} \succeq 0$, and $t \in \mathcal{T} \setminus \{t_{\mathrm{F}}\}$,

$$g_t^{\mathrm{l}}\left(\boldsymbol{\lambda}_t^{\mathrm{l}}\right) \leq \min_{\boldsymbol{s}\in\mathcal{S},\boldsymbol{r}\in\mathcal{R}} E_t^{\mathrm{l}}, \quad g_t^{\mathrm{u}}\left(\boldsymbol{\lambda}_t^{\mathrm{u}}\right) \geq \max_{\boldsymbol{s}\in\mathcal{S},\boldsymbol{r}\in\mathcal{R}} E_t^{\mathrm{u}}. \tag{44}$$

Thus, the proposition trivially holds. □

Since the Lagrange dual functions $g_t^{\mathrm{l}}\left(\boldsymbol{\lambda}_t^{\mathrm{l}}\right)$ and $g_t^{\mathrm{u}}\left(\boldsymbol{\lambda}_t^{\mathrm{u}}\right)$ are linear within a feasible polyhedron set, the inequalities (41)-(43) can be incorporated as a set of linear constraints into the optimization problem.

B. Cost function

The energy charge J^{E}, demand charge J^{DC}, and the BESS degradation cost J^{BD} are dependent of the BESS's net power consumption P_t^{N}, and hence dependent of the uncertainties $\boldsymbol{s}$ and $\boldsymbol{r}$. However, it is non-trivial to get the closed-form solution of the maximums of those costs with respect to $\boldsymbol{s}$ and $\boldsymbol{r}$. To remove the dependency of the costs on s_t and r_t, we leverage approximations that are computed under the assumption that s_t and r_t are equal to their nominal values $\tilde{s}_t$, $\tilde{r}_t$; the nominal values can be the average values of frequency regulation signal and the utilized synchronized reserves in historical data. Then, we calculate the BESS's power and SoC under the nominal values, which are indicated with tildes on them, as follows

$$0 \leq \tilde{P}_t^{\mathrm{C}} \leq \tilde{\mu}_t \overline{P}^{\mathrm{C}} \qquad \forall t \in \mathcal{T} \tag{45}$$

$$0 \leq \tilde{P}^{\mathrm{D}} \leq (1-\tilde{\mu}_t)\,\overline{P}^{\mathrm{D}} \qquad \forall t \in \mathcal{T} \tag{46}$$

$$\tilde{E}_1^{\mathrm{B}} = E_1^{\mathrm{B}} \tag{47}$$

$$\tilde{E}_{t+1}^{\mathrm{B}} = \tilde{E}_t^{\mathrm{B}} + \eta_c \tilde{P}_t^{\mathrm{C}} - \frac{1}{\eta_d}\tilde{P}_t^{\mathrm{D}} \qquad \forall t \in \mathcal{T} \tag{48}$$

$$\tilde{P}_t^{\mathrm{N}} = \begin{cases} P_t^{\mathrm{B}} - \tilde{s}_t P_t^{\mathrm{FR}} - \tilde{r}_t P_t^{\mathrm{SR}} & \text{if } t \in \mathcal{T}_{\mathrm{S}} \\ \frac{\overline{E} - \tilde{E}_{t_{\mathrm{F}}-1}}{\eta_c} & \text{if } t = t_{\mathrm{F}} - 1 \\ -\overline{P}^{\mathrm{D}} & \text{if } t \in \mathcal{T}_{\mathrm{F}} \end{cases} \tag{49}$$

$$\tilde{P}_t^{\mathrm{G}} = \tilde{P}_t^{\mathrm{N}} + P_t^{\mathrm{UC}} - P_t^{\mathrm{PV}} \qquad \forall t \in \mathcal{T} \tag{50}$$

Using these nominal values, we get the cost approximations as follows

$$\tilde{J}^{\mathrm{E}} = \pi^{\mathrm{E}} \sum_{t=1}^{T} \tilde{P}_t^{\mathrm{G}} \cdot \Delta t \tag{51}$$

$$\tilde{J}^{\mathrm{DC}} = \pi^{\mathrm{DC}} \max_{t=1,\ldots,T} \tilde{P}_t^{\mathrm{G}} \tag{52}$$

$$\tilde{J}^{\mathrm{BD}} = \pi^{\mathrm{BD}} \sum_{t=1}^{T} |\tilde{P}_t^{\mathrm{N}}|. \tag{53}$$

which does not depend on $\boldsymbol{s}$ and $\boldsymbol{r}$.

Note that $\tilde{P}_t^{\mathrm{G}}$ is still uncertain since it depends on P_t^{UC} and P_t^{PV}, and hence the approximated energy charge $\tilde{J}^{\mathrm{E}}$ and demand charge $\tilde{J}^{\mathrm{DC}}$ depend on $\boldsymbol{P}^{\mathrm{PV}}$ and $\boldsymbol{P}^{\mathrm{UC}}$. It is obvious that $\tilde{J}^{\mathrm{E}}$ and $\tilde{J}^{\mathrm{DC}}$ are at their maximum with minimum PV generation and maximum load. Thus, the maximum of the sum of $\tilde{J}^{\mathrm{E}}$ and $\tilde{J}^{\mathrm{DC}}$ is given

$$\begin{aligned} \tilde{J}^{\max} &= \max_{\boldsymbol{P}^{\mathrm{PV}},\boldsymbol{P}^{\mathrm{UC}}} \pi^{\mathrm{E}} \sum_{t=1}^{T} \tilde{P}_t^{\mathrm{G}} \cdot \Delta t + \pi^{\mathrm{DC}} \max_{t\in\mathcal{T}} \tilde{P}_t^{\mathrm{G}} \\ &= \pi^{\mathrm{E}} \left(\sum_{t=1}^{T} \tilde{P}_t^{\mathrm{N}} + \overline{\Gamma}_T^{\mathrm{UC}} - \underline{\Gamma}_T^{\mathrm{PV}} \right) \Delta t \\ &\quad + \pi^{\mathrm{DC}} \max_{t\in\mathcal{T}} \left(\tilde{P}_t^{\mathrm{N}} + \overline{P}_t^{\mathrm{UC}} - \underline{P}_t^{\mathrm{PV}} \right). \end{aligned} \tag{54}$$

Thus, the approximated total cost $\tilde{J}^{\mathrm{T}}$ is defined as follows

$$\tilde{J}^{\mathrm{T}} = \tilde{J}^{\max} - J^{\mathrm{AC}} + \tilde{J}^{\mathrm{BD}}. \tag{55}$$

C. Reformulation

Combining the results above, we reformulate the robust look-ahead algorithm as follows

$$\begin{aligned} \min_{\boldsymbol{y}} \ & \tilde{J}^{\mathrm{T}} \\ \text{s.t.} \ & (13)-(18), (33)-(35) \\ & (41)-(43), (45)-(50) \end{aligned} \tag{56}$$

where the vector of the decision variables are as follows

$$\begin{aligned} \boldsymbol{y} = \Big(& (P_t^{\mathrm{B}}, P_t^{\mathrm{FR}}, P_t^{\mathrm{SR}}, \alpha_t, \beta_t)_{t\in\mathcal{T}_{\mathrm{S}}}, \\ & (\tilde{E}_{t+1}^{\mathrm{B}}, \tilde{P}_t^{\mathrm{C}}, \tilde{P}_t^{\mathrm{D}}, \tilde{P}_t^{\mathrm{N}}, \tilde{\mu}_t)_{t\in\mathcal{T}}, \\ & (\boldsymbol{\lambda}_t^{\mathrm{l}}, \boldsymbol{\lambda}_t^{\mathrm{u}})_{t\in\mathcal{T}\setminus\{t_{\mathrm{F}}\}} \Big) \end{aligned} \tag{57}$$

Theorem 1. *The optimal solution* $\boldsymbol{x}^* = \{P_t^{B*}, P_t^{FR*}, P_t^{SR*}, \alpha_t^*, \beta_t^*\}_{t\in\mathcal{T}_S}$ *obtained from the robust look-ahead* (56) *is feasible for the original problem* (29).

Proof. The constraints (2) and (3) trivially hold for all $\boldsymbol{w}$ in $\mathcal{W}$ by the constraints (4)-(6), (16)-(18). Thus, it is sufficient to show that (7) and (12) holds for all with the obtained solution $\boldsymbol{x}^*$ for all $\boldsymbol{w}$ in $\mathcal{W}$.

The optimal Lagrange multipliers $\boldsymbol{\lambda}_t^{\mathrm{l}*}$ and $\boldsymbol{\lambda}_t^{\mathrm{u}*}$ satisfy $g_t^{\mathrm{l}}(\boldsymbol{\lambda}_t^{\mathrm{l}*}) \geq 0$, $g_t^{\mathrm{u}}(\boldsymbol{\lambda}_t^{\mathrm{u}*}) \geq 0$, $\boldsymbol{\lambda}_t^{\mathrm{l}*} \succeq 0$, and $\boldsymbol{\lambda}_t^{\mathrm{u}*} \succeq 0$. Hence, by Proposition 2, the inequalities (38), (39) hold. Since these is a sufficient condition for the original robust constraint (30), (31), the constraint (7) holds for $\boldsymbol{w} \in \mathcal{W}$. Similarly, (12) holds for all possible uncertainties $\boldsymbol{w} \in \mathcal{W}$. Thus, the statement of the theorem holds. □

Note that all the objectives and constraints are linear except $|\tilde{P}_t^{\mathrm{N}}|$ in (53) and $\max_{t\in\mathcal{T}}\left(\tilde{P}_t^{\mathrm{N}} + \overline{P}_t^{\mathrm{UC}} - \underline{P}_t^{\mathrm{PV}}\right)$ in (54).To reformulate it into an equivalent Mixed-Integer Linear Programming (MILP) problem, we alternate $|\tilde{P}_t^{\mathrm{N}}|$ and $\max_{t\in\mathcal{T}}\left(\tilde{P}_t^{\mathrm{N}} + \overline{P}_t^{\mathrm{UC}} - \underline{P}_t^{\mathrm{PV}}\right)$ to auxiliary variables z_t and u, respectively. Then, we add the following constraints to (56)

$$z_t \geq \tilde{P}_t^{\mathrm{N}}, \ \ z_t \geq -\tilde{P}_t^{\mathrm{N}} \qquad \forall t \in \mathcal{T} \tag{58}$$

$$u \geq \tilde{P}_t^{\mathrm{N}} + \overline{P}_t^{\mathrm{UC}} - \underline{P}_t^{\mathrm{PV}} \qquad \forall t \in \mathcal{T}. \tag{59}$$

The optimal solutions of (56) determines the battery's power at each sub-interval. Suppose that $P_t^{\mathrm{B}*}$, $P_t^{\mathrm{FR}*}$, $P_t^{\mathrm{SR}*}$

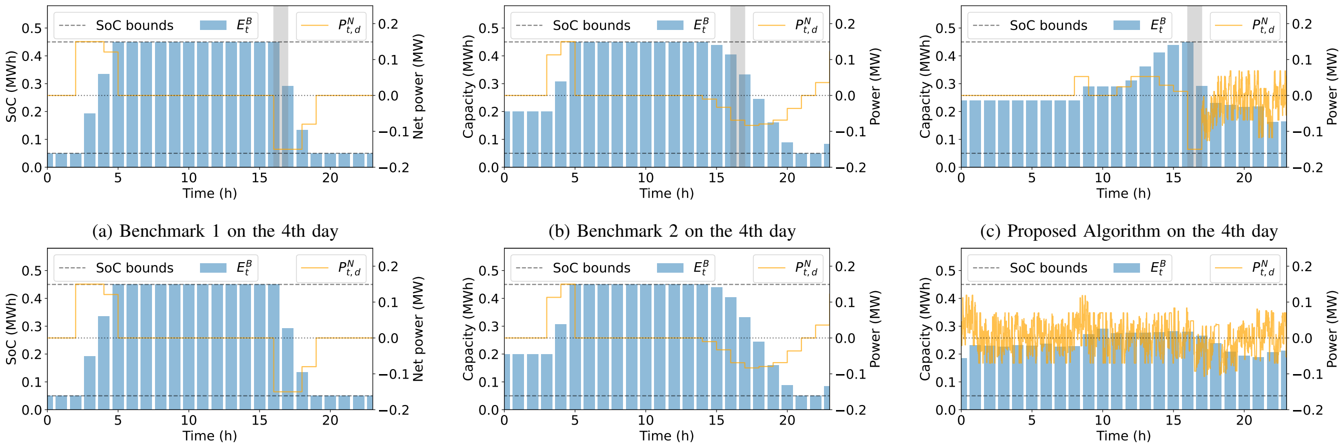

(a) Benchmark 1 on the 4th day (b) Benchmark 2 on the 4th day (c) Proposed Algorithm on the 4th day

(d) Benchmark 1 (e) Benchmark 2 on the 7th day (f) Proposed Algorithm on the 7th day

Fig. 1: BESS's SoC E_t^{B} and net power $P_{t,d}^{\mathrm{N}}$ on the 4th and 7th days of the month, where the grey block corresponds to $\mathcal{T}_{\mathrm{F}}$ when the full capacity of BESS is called by ISO.

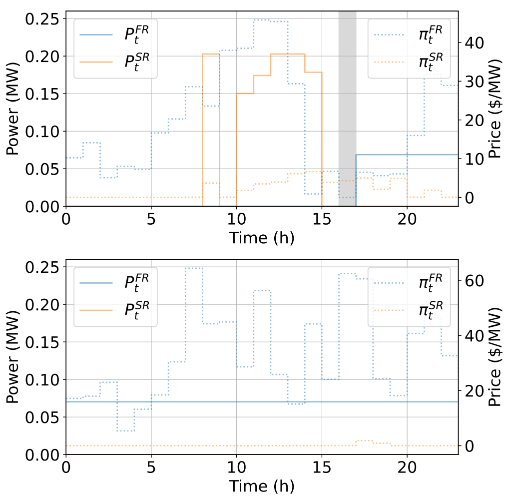

Fig. 2: Offered reserves to the ancillary service markets on the 4th day (top) and the 7th day (bottom).

are the obtained optimal solutions, $s_{t,d}$ and $r_{t,d}$ are the real-time regulation signal at each sub-interval. Then, the real-time net charging power of the BESS at each sub-interval is determined as follows

$$P_{t,d}^{\mathrm{N}} = \begin{cases} \left(P_t^{\mathrm{B}*} - s_{t,d} P_t^{\mathrm{FR}*} - r_{t,d} P_t^{\mathrm{SR}*}\right)^+ & \text{if } t \in \mathcal{T}_{\mathrm{S}} \\ \frac{\overline{E}^{\mathrm{B}} - E_{t_{\mathrm{F}}-1}}{\eta_c} & \text{if } t = t_{\mathrm{F}} - 1 \\ -\overline{P}^{\mathrm{D}} & \text{if } t \in \mathcal{T}_{\mathrm{F}} \end{cases} \tag{60}$$

IV. Experiments

In this section, we compare our proposed algorithms with two benchmarks. We run each algorithm for a month with 29 days and compare the monthly energy charge of them.

We assume that the total capacity of the BESS is 0.5MWh, the maximum charging and charging powers are $\overline{P}^{\mathrm{C}} = \overline{P}^{\mathrm{D}} = 0.15$ MW , the bounds on SoC are $\underline{E}^{\mathrm{B}} = 0.05$ MWh and $\overline{E}^{\mathrm{B}} = 0.45$ MWh, and the efficiencies are $\eta_c = \eta_d = 0.95$. We assume that the energy cost per unit power is $\pi^{\mathrm{E}} = 61.82$ \$/MWh, the coefficient of the maximum power is $\pi^{\mathrm{DC}} = 300$ \$/MW, the number of cycle operation is $N_{\mathrm{cyc}} = 20,000$ and the price of the battery cell is $\pi^{\mathrm{Cell}} = \$100,000$. The bounds and nominal values of the frequency regulation signal $\underline{s} = -0.82$, $\overline{s} = 0.7$, $\tilde{s} = 0$ and utilized synchronized reserve $\underline{r} = 0$, $\overline{r} = 0.5$, $\tilde{r} = 0.001$ are derived from the PJM's regulation data in 2020 [21]. The uncertainty budgets $\underline{\Gamma}_t^{\mathrm{s}}$, $\overline{\Gamma}_t^{\mathrm{s}}$, and $\underline{\Gamma}_t^{\mathrm{r}}$, $\overline{\Gamma}_t^{\mathrm{r}}$ are derived from the minimum and maximum cumulative sum from the same data. We leverage solar radiation data from SoDa [22] to generate prediction $\underline{P}_t^{\mathrm{PV}}$ and $\overline{P}_t^{\mathrm{PV}}$. The prediction on building's load and P_t^{PV} is obtained by scaling hourly load data from PJM [23] into a building load scale. Then, we sample P_t^{PV} and P_t^{UC} from uniform distributions over ranges $[\underline{P}_t^{\mathrm{PV}}, \overline{P}_t^{\mathrm{PV}}]$ and $[\underline{P}_t^{\mathrm{UC}}, \overline{P}_t^{\mathrm{UC}}]$, respectively. The monthly average value of P_t^{PV} and P_t^{UC} are 55 kW and 417 kW, respectively. The uncertainty budgets $\underline{\Gamma}_t^{\mathrm{PV}}$,$\overline{\Gamma}_t^{\mathrm{PV}}$, $\underline{\Gamma}_t^{\mathrm{UC}}$,$\overline{\Gamma}_t^{\mathrm{UC}}$ are chosen as appropriate values. For the prices of the ancillary service markets π_t^{FR} and π_t^{SR}, we use the PJM's frequency regulation market and day-ahead synchronized reserve market from June 18th 2023 to July 16th 2023. We assume that full BESS capacity is called on 4th day on 4pm and 21st day on 19pm.

We compare the proposed algorithm with two benchmarks. FBenchmark 1 is a rule-based BESS controller which fully discharges the BESS during $\mathcal{T}_{\mathrm{F}}$ if there is an anticipated call from the ISO, or 4 pm- 7 pm otherwise, and fully charges from 2 am to 5 am every day. Benchmark 2 is a deterministic optimization algorithm that does not consider ancillary service markets:

$$\begin{aligned} \min_{P_t^{\mathrm{C}}, P_t^{\mathrm{D}}, P_t^{\mathrm{N}}, \mu_t, E_t^{\mathrm{B}}} \quad & J^E + J^{\mathrm{DC}} + J^{\mathrm{BD}} \\ \text{s.t.} \quad & (1) - (8) \qquad \forall t \in \mathcal{T} \\ & (9) - (12) \end{aligned} \tag{61}$$

Since the BESS does not provide any ancillary services, there is no uncertainty within the BESS's SoC and the objective

TABLE I: Costs of Each Algorithm

	Benchmark 1	Benchmark 2	Proposed Algorithm
J^{T} ($)	$18,670	$18,450	$17,850
J^{E}	$15,690	$15,700	$15,660
J^{DC} ($)	$2,940	$2,730	$3,020
J^{AC} ($)	-	-	$830
J^{BD} ($)	$71.94	$65.52	$41.75

function is deterministic. This benchmark aims to observe how much profit we can additionally get from the ancillary service markets by our proposed algorithm.

Table I demonstrates the costs under each algorithm, Fig. 1 illustrates the BESS's SoC E_t^{B} and net power $P_{t,d}^{\mathrm{N}}$ on the 4th day, when there was a call by the ISO, and the 7th day when there were not. Overall, the total cost J^{T} in the proposed algorithm is much lower than the benchmarks. The demand charge J^{DC} is higher in our proposed algorithm since, as can be seen in Fig. 1c, the battery provides ancillary services during the period of high load (4pm - 7pm), and hence the maximum power consumption becomes higher than the benchmarks. However, the revenues from the ancillary service markets J^{AC} remains a lot even after offsets the demand charge. Also, the BESS's SoC cycles less in our proposed algorithm so that the battery degradation cost was the lowest.

Fig. 2 shows the offers to the ancillary service markets by the proposed algorithm. Before there is an anticipated call by the ISO on the 4th day, it does not provide the frequency regulation to prepare for the ISO's call, while providing synchronized reserve service for several hours. On the other hand, the proposed algorithm makes an offer to the frequency regulation market every hour on the 7th day to maximize the revenue; it is because the price from frequency regulation is higher than providing synchronized reserve.

Last but not least, we verified that the bounds on the BESS's SoC E_t (7) under our proposed algorithm hold for all the time steps, which shows the robustness of it.

V. Conclusion

In this paper, we proposed a robust look-ahead battery bidding algorithm for participation in frequency regulation and synchronized reserve markets in cases where the BESS has been committed to a long-term capacity market. The proposed algorithm makes bids to the frequency regulation market and synchronized reserve markets in a way that it never violates any operational constraints for any possible uncertainties within the defined plausible uncertainty sets. To reduce the conservatism within the uncertainties, we leverage the uncertainty budget in defining the correspondence uncertainty sets. We reformulate the robust optimization algorithm into a feaisble MILP problem by using the Lagrange dual functions. Numerical experiments show the robustness of our proposed algorithm as well as it has outperformed two benchmarks.

Appendix

A. Lagrange dual functions

The Lagrange dual functions $g_t^{\mathrm{l}}(\boldsymbol{\lambda}_t^{\mathrm{l}})$ of $\min_{\boldsymbol{s}\in\mathcal{S},\boldsymbol{r}\in\mathcal{R}} E_t^{\mathrm{l}}$ can be derived as follows

$$\begin{aligned} g_t^{\mathrm{l}}\left(\boldsymbol{\lambda}_t^{\mathrm{l}}\right) = \inf_{\boldsymbol{s},\boldsymbol{r}}\ & E_t^{\mathrm{init}} + \sum_{k=i(t)}^{t-1} \eta_c \left(P_k^{\mathrm{B}} - s_k P_k^{\mathrm{FR}} - r_k P_k^{\mathrm{SR}}\right) \\ & - \sum_{k=i(t)}^{t-1} \left(\frac{1}{\eta_d} - \eta_c\right) P_k^{\mathrm{Du}} + \sum_{k=1}^{t-1} \Bigg(\lambda_{t,k}^{\mathrm{l},1}\left(-s_k + \underline{s}\right) + \lambda_{t,k}^{\mathrm{l},2}\left(s_k - \overline{s}\right) \\ & + \lambda_{t,k}^{\mathrm{l},3}\left(-\sum_{l=1}^{k} s_l + \underline{\Lambda}_k^{\mathrm{s}}\right) + \lambda_{t,k}^{\mathrm{l},4}\left(\sum_{l=1}^{k} s_l - \overline{\Lambda}_k^{\mathrm{s}}\right) \\ & + \lambda_{t,k}^{\mathrm{l},5}\left(-r_k + \underline{r}\right) + \lambda_{t,k}^{\mathrm{l},6}\left(r_k - \overline{r}\right) \\ & + \lambda_{t,k}^{\mathrm{l},7}\left(-\sum_{l=1}^{k} r_l + \underline{\Lambda}_k^{\mathrm{r}}\right) + \lambda_{t,k}^{\mathrm{l},8}\left(\sum_{l=1}^{k} r_l - \overline{\Lambda}_k^{\mathrm{r}}\right)\Bigg) \end{aligned} \tag{62}$$

where $\lambda_{t,k}^{\mathrm{l},j}$ are the Lagrange multipliers composing $\boldsymbol{\lambda}_t^{\mathrm{l}}$, and E_t^{init} and $i(t)$ are defined as follows.

$$E_t^{\mathrm{init}} = \begin{cases} E_1^{\mathrm{B}} & \text{if } t < t_{\mathrm{F}} \\ \overline{E}^{\mathrm{B}} & \text{if } t \geq t_{\mathrm{F}} \end{cases}, \quad i(t) = \begin{cases} 1 & \text{if } t < t_{\mathrm{F}} \\ t_{\mathrm{F}} & \text{if } t \geq t_{\mathrm{F}}. \end{cases} \tag{63}$$

Considering that $g_t^{\mathrm{l}}(\boldsymbol{\lambda}_t^{\mathrm{l}})$ is equal to $-\infty$ if one of the coefficients of s_k and r_k is non-zero, we get the following

$$g_t^{\mathrm{l}}\left(\boldsymbol{\lambda}_t^{\mathrm{l}}\right) = \begin{cases} E_t^{\mathrm{init}} + \sum_{k=i(t)}^{t-1} \eta_c P_k^{\mathrm{B}} & \\ \quad - \left(\frac{1}{\eta_d} - \eta_c\right) P_k^{\mathrm{Du}} + \Omega_t^{\mathrm{l}} & \text{if } \boldsymbol{\lambda}_t^{\mathrm{l}} \in \Lambda_t^{\mathrm{l}} \\ -\infty & \text{otherwise} \end{cases} \tag{64}$$

where Ω_t^{l} and Λ_t^{l} are defined as follows

$$\begin{aligned} \Omega_t^{\mathrm{l}} = \sum_{k=i(t)}^{t-1} & \lambda_{t,k}^{\mathrm{l},1}\underline{s} - \lambda_{t,k}^{\mathrm{l},2}\overline{s} + \lambda_{t,k}^{\mathrm{l},3}\underline{\Lambda}_k^{\mathrm{s}} - \lambda_{t,k}^{\mathrm{l},4}\overline{\Lambda}_k^{\mathrm{s}} \\ & + \lambda_{t,k}^{\mathrm{l},5}\underline{r} - \lambda_{t,k}^{\mathrm{l},6}\overline{r} + \lambda_{t,k}^{\mathrm{l},7}\underline{\Lambda}_k^{\mathrm{r}} - \lambda_{t,k}^{\mathrm{l},8}\overline{\Lambda}_k^{\mathrm{r}} \end{aligned} \tag{65}$$

$$\begin{aligned} \Lambda_t^{\mathrm{l}} := \Bigg\{ \boldsymbol{\lambda}_t^{\mathrm{l}} \ \Bigg|\ & -\eta P_k^{\mathrm{FR}} - \lambda_{t,k}^{\mathrm{l},1} + \lambda_{t,k}^{\mathrm{l},2} - \sum_{l=k}^{t-1} \lambda_{t,l}^{\mathrm{l},3} - \lambda_{t,l}^{\mathrm{l},4} = 0 \\ & -\eta P_k^{\mathrm{SR}} - \lambda_{t,k}^{\mathrm{l},5} + \lambda_{t,k}^{\mathrm{l},6} - \sum_{l=k}^{t-1} \lambda_{t,l}^{\mathrm{l},7} - \lambda_{t,l}^{\mathrm{l},8} = 0 \\ & \forall k \in \{i(t), \dots, t-1\} \\ & -\lambda_{t,k}^{\mathrm{l},1} + \lambda_{t,k}^{\mathrm{l},2} - \sum_{l=1}^{k} \lambda_{t,l}^{\mathrm{l},3} - \lambda_{t,l}^{\mathrm{l},4} = 0 \\ & -\lambda_{t,k}^{\mathrm{l},5} + \lambda_{t,k}^{\mathrm{l},6} - \sum_{l=1}^{k} \lambda_{t,l}^{\mathrm{l},7} - \lambda_{t,l}^{\mathrm{l},8} = 0 \forall k \in \{1, \dots, i(t)-1\} \Bigg\} \end{aligned}$$

Likewise, the function $g_t^{\mathrm{u}}(\lambda_t^{\mathrm{u}})$ is given as follows

$$g_t^{\mathrm{u}}\left(\boldsymbol{\lambda}_t^{\mathrm{u}}\right) = \begin{cases} E_t^{\mathrm{init}} + \sum_{k=i(t)}^{t-1} \eta P_k^{\mathrm{B}} + \Omega_t^{\mathrm{u}} & \text{if } \boldsymbol{\lambda}_t^{\mathrm{u}} \in \Lambda_t^{\mathrm{u}} \\ -\infty & \text{otherwise} \end{cases} \tag{66}$$

where Ω_t^{u} and Λ_t^{u} are defined as (65) and (66) with $\lambda_{t,k}^{\mathrm{l},j}$ alternated to $-\lambda_{t,k}^{\mathrm{u},j}$ and η_c alternated to η.

References

[1] B. Xu, Y. Wang, Y. Dvorkin, R. Fernández-Blanco, C. A. Silva-Monroy, J.-P. Watson, and D. S. Kirschen, “Scalable planning for energy storage in energy and reserve markets,” *IEEE Transactions on Power systems*, vol. 32, no. 6, pp. 4515–4527, 2017.

[2] K. Meng, Z. Y. Dong, Z. Xu, Y. Zheng, and D. J. Hill, “Coordinated dispatch of virtual energy storage systems in smart distribution networks for loading management,” *IEEE Transactions on Systems, Man, and Cybernetics: Systems*, vol. 49, no. 4, pp. 776–786, 2017.

[3] H. J. Kim, R. Sioshansi, and A. J. Conejo, “Benefits of stochastic optimization for scheduling energy storage in wholesale electricity markets,” *Journal of Modern Power Systems and Clean Energy*, vol. 9, no. 1, pp. 181–189, 2020.

[4] K. Garifi, K. Baker, B. Touri, and D. Christensen, “Stochastic model predictive control for demand response in a home energy management system,” in *2018 IEEE power & energy society general meeting (PESGM)*. IEEE, 2018, pp. 1–5.

[5] R. H. Byrne, R. J. Concepcion, and C. A. Silva-Monroy, “Estimating potential revenue from electrical energy storage in pjm,” in *2016 IEEE Power and Energy Society General Meeting (PESGM)*. IEEE, 2016, pp. 1–5.

[6] G. He, Q. Chen, C. Kang, Q. Xia, and K. Poolla, “Cooperation of wind power and battery storage to provide frequency regulation in power markets,” *IEEE Transactions on Power Systems*, vol. 32, no. 5, pp. 3559–3568, 2016.

[7] S. Hanif, M. J. E. Alam, K. Roshan, B. A. Bhatti, and J. C. Bedoya, “Multi-service battery energy storage system optimization and control,” *Applied Energy*, vol. 311, p. 118614, 2022.

[8] Y. Shi, B. Xu, D. Wang, and B. Zhang, “Using battery storage for peak shaving and frequency regulation: Joint optimization for superlinear gains,” *IEEE Transactions on Power Systems*, vol. 33, no. 3, pp. 2882–2894, 2017.

[9] G. Araujo, *Multiple Market Participation of Battery Storage System.* Ph.D. dissertation, Aalborg Universitet, 2019.

[10] A. A. Thatte, L. Xie, D. E. Viassolo, and S. Singh, “Risk measure based robust bidding strategy for arbitrage using a wind farm and energy storage,” *IEEE Transactions on Smart Grid*, vol. 4, no. 4, pp. 2191–2199, 2013.

[11] J. Kim, Y. Choi, S. Ryu, and H. Kim, “Robust operation of energy storage system with uncertain load profiles,” *Energies*, vol. 10, no. 4, p. 416, 2017.

[12] Y. Huang, L. Wang, W. Guo, Q. Kang, and Q. Wu, “Chance constrained optimization in a home energy management system,” *IEEE Transactions on Smart Grid*, vol. 9, no. 1, pp. 252–260, 2016.

[13] M. Farahani, A. Samimi, and H. Shateri, “Robust bidding strategy of battery energy storage system (bess) in joint active and reactive power of day-ahead and real-time markets,” *Journal of Energy Storage*, vol. 59, p. 106520, 2023.

[14] Y. Ji, Q. Xu, J. Zhao, Y. Yang, and L. Sun, “Day-ahead and intra-day optimization for energy and reserve scheduling under wind uncertainty and generation outages,” *Electric Power Systems Research*, vol. 195, p. 107133, 2021.

[15] H. Zhang, Z. Hu, E. Munsing, S. J. Moura, and Y. Song, “Data-driven chance-constrained regulation capacity offering for distributed energy resources,” *IEEE Transactions on Smart Grid*, vol. 10, no. 3, pp. 2713–2725, 2018.

[16] Y. Guo and Y. Fang, “Electricity cost saving strategy in data centers by using energy storage,” *IEEE Transactions on Parallel and Distributed Systems*, vol. 24, no. 6, pp. 1149–1160, 2012.

[17] M. A. Ortega-Vazquez, “Optimal scheduling of electric vehicle charging and vehicle-to-grid services at household level including battery degradation and price uncertainty,” *IET Generation, Transmission & Distribution*, vol. 8, no. 6, pp. 1007–1016, 2014.

[18] B. Xu, A. Oudalov, A. Ulbig, G. Andersson, and D. S. Kirschen, “Modeling of lithium-ion battery degradation for cell life assessment,” *IEEE Transactions on Smart Grid*, vol. 9, no. 2, pp. 1131–1140, 2016.

[19] N. Nazir and M. Almassalkhi, “Guaranteeing a physically realizable battery dispatch without charge-discharge complementarity constraints,” *IEEE Transactions on Smart Grid*, 2021.

[20] S. P. Boyd and L. Vandenberghe, *Convex optimization*. Cambridge university press, 2004.

[21] PJM, “RTO regulation signal data for 2020.xls,” https://www.pjm.com/markets-and-operations/ancillary-services.aspx, accessed: 2023-06-28.

[22] L. Wald, M. Albuisson, C. Best, C. Delamare, D. Dumortier, E. Gaboardi, A. Hammer, D. Heinnemann, R. Kift, S. Kunz, *et al.*, “Soda: a project for the integration and exploitation of networked solar radiation databases.” in *Environmental Communication in the Information Society*. International Society for Environmental Protection, Vienna, Austria, 2002, pp. 713–720.

[23] PJM, “Data miner,” https://dataminer2.pjm.com/list, accessed: 2023-06-20.